BCSJ

Document type: Article

Kinetically Protected Carbon-Bridged Oligo(*p*-phenylenevinylene) Derivatives for Blue Color Amplified Spontaneous Emission

Víctor Bonal,[1] Marta Morales-Vidal,[2] Pedro G. Boj,[2] José M. Villalvilla,[1] José A. Quintana,[2] Naiti Lin,[3] Shoya Watanabe,[4] Hayato Tsuji,*[4] Eiichi Nakamura,*[3] and María A. Díaz-García*[1]

[1]Departamento de Física Aplicada and Instituto Universitario de Materiales de Alicante, Universidad de Alicante, Alicante 03080, Spain

[2]Departamento de Óptica, Farmacología y Anatomía and Instituto Universitario de Materiales de Alicante, Universidad de Alicante, Alicante 03080, Spain

[3]Department of Chemistry, School of Science, The University of Tokyo, Hongo, Bunkyo-ku, Tokyo 113-0033, Japan

[4]Department of Chemistry, Faculty of Science, Kanagawa University, 2946 Tsuchiya, Hiratsuka, Kanagawa 259-1293, Japan

E-mail: tsujiha@kanagawa-u.ac.jp (H. Tsuji), nakamura@chem.s.u-tokyo.ac.jp (E. Nakamura), maria.diaz@ua.es (M. A. Díaz-García)

Received: February 12, 2020; Accepted: March 19, 2020; Web Released: March 27, 2020

Hayato Tsuji

Hayato Tsuji received his doctor of engineering degree in 2001 at Kyoto University. He worked as a Research Fellow (PD) of JSPS, and was appointed to assistant professor at Institute for Chemical Research, Kyoto University in 2002, associate professor at the University of Tokyo in 2006, and full professor at Kanagawa University in 2016. He concurrently worked as a PRESTO researcher for "New Materials Science and Elemental Strategy" (2011–15), and visiting professor at University of Strasbourg, France (2012–13). His current research interest is synthetic chemistry for creating functional materials that are useful for biological and aqueous environmental conditions.

Eiichi Nakamura

Eiichi Nakamura is the University Professor in the Office of the President and the Department of Chemistry of The University of Tokyo, and a member of the Science Council of Japan. He works in a diverse field of synthetic and physical chemistry of organic and inorganic matter, with a focus on their functions. In 2007, he introduced atomic resolution transmission electron microscopy for the study of molecular motions and reactions at the single-molecule level. His research activities have been recognized through several awards and honors, including the Medal of Honor with Purple Ribbon awarded by His Majesty the Emperor (2009). He was elected an Honorary Foreign Member of the American Academy of Arts and Sciences in 2008.

María Ángeles Díaz-García

María A. Díaz-García received the Ph.D. in Physics in 1995 at the Autonomus Uni-versity of Madrid, Spain, working on nonlinear optics. As a postdoctoral researcher, she was part of the pioneer group of Prof. Heeger, at the Univ. of California in Santa Barbara, USA, which discovered stimulated emission in semiconducting polymers in 1996. She also performed postdoctoral work with Prof. W.E. Moerner at the Univ. of California, San Diego. She joined the faculty of the University of Alicante in 2001, where she founded the "Organic Electronics and Photonics" group, which leads since then. She was appointed full professor in 2010. Her latest research focusses on organic optoelectronic materials and devices, with major emphasis on organic lasers.

Abstract

Carbon-bridged oligo(*p*-phenylenevinylene)s (COPV*n* with repeating unit $n = 1$–6) have demonstrated great success as laser dyes for thin-film organic lasers. The excellent photostability observed in the longer homologues is, however, not present in the blue-emitting shorter compounds COPV1 and COPV2, attributed to the unprotected terminal positions that can degrade by photoreaction in the excited state. Here we report the syn-

thesis of various COPV1 and COPV2 derivatives functionalized at the terminal positions with two types of sterically bulky protecting substituents: Tip (2,4,6-triisopropylphenyl) and *tert*-butyl (*t*-Bu) groups. Such molecular designs aim at preventing such photodegradation processes and thus to improve their stability. The efficacy of kinetic isotope effect for stabilization is also examined for COPV2, by the addition at terminal positions of deuterium atoms. Absorption, photoluminescence (PL), including PL quantum yield, and amplified spontaneous emission (ASE) studies have been conducted in polystyrene films doped with each of the derivatives. Significant and slight improvements of the ASE photostability are observed for the compounds with Tip groups and deuterium, respectively. Installation of substituents slightly affects the ASE wavelength within the blue spectral region, that is 385–413 nm and 462–474 nm, for COPV1 and COPV2, respectively.

Keywords: Phenylenevinylene | Kinetic stabilization | Laser

1. Introduction

During the last decade many efforts have been devoted to the design and synthesis of new organic materials, such as small molecules, oligomers, polymers and dendrimers, with efficient properties to be used as the active units in optoelectronic devices, such as transistors, solar cells, light-emitting diodes and lasers.[1–5] Particularly, for low-cost and integrable thin-film organics lasers, solution processable compounds showing simultaneously very large photoluminescence quantum yields (PLQY), both in solution and thin film, and a high chemical and photostability, are pursued.[6–8]

Phenylenevinylene (PV)-based materials are among the most extensively investigated materials for organic electronics. For laser applications, the first demonstrations of laser action on semiconducting materials occurred on poly(phenylenevinylenes) (PPVs) such as MEH-PPV.[9,10] Later on, other PV-based polymers and oligomers (OPVs) were developed for these and other purposes.[2–4,11–15] Recently, fused and planar OPV derivatives have been prepared by inserting carbon bridges between the phenylene and vinylene units, thus providing carbon-bridged oligo(*p*-phenylenevinylene)s (COPVs).[16–18] These compounds proved to be more responsive to doping and photoexcitation, such as intense light absorption and high PLQY reaching 100%, and also to be much more stable than the conventional *p*-phenylenevinylenes, due to steric protection of the middle part of the molecules with aryl and/or phenyl substituents on the bridging carbon atoms. Taking advantage of these properties, we have demonstrated excellent lasing properties using COPVs dispersed in polystyrene (PS) films.[7,16] A remarkable feature of COPV*n* with respect to other types of oligomers,[19] polymers,[20] and dyes,[21,22] is the possibility to tune the laser wavelength output over a wide range of the visible spectrum by changing the repeating unit *n*. Particularly, COPV*n* compounds with $n \geq 3$ have exceptionally high photostabilities and low pump laser thresholds.[7] On the other hand, the shorter homologues, COPV1 and COPV2, emitting blue color, show a somewhat limited performance, mainly in terms of photostability, most likely due to the reactive terminal sites in the photoexcited states.[17,23] A possible strategy to improve the photostability of these short homologues is to reduce the number of reactive sites through expansion of conjugation in terms of ring fusion or polymerization to delocalize the exciton (thermodynamic stabilization).[24–26] Indeed, this strategy has been successful in improving the photostability in the short COPV-based lasers, but the emission color significantly shifted to green because of the extension of conjugation. To keep the emission color blue, we envisioned that the kinetic stabilization by introducing protecting groups into the reactive terminal positions may be effective.

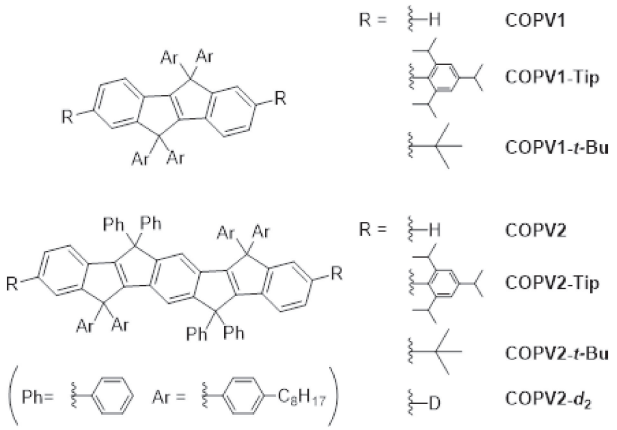

Figure 1. Chemical structures of COPV1 and COPV2 derivatives.

Here, we report the synthesis and optical characterization (absorption, photoluminescence and amplified spontaneous emission, ASE) of PS films doped with various COPV1 and COPV2 derivatives with protecting substituents at the terminal positions. The compounds used in the present study are **COPV1-Tip, COPV1-*t*-Bu, COPV2-Tip, COPV2-*t*-Bu and COPV2-d_2** (see chemical structures in Figure 1). Compounds were designed to prevent chemical and photodegradation, while keeping the robust all-carbon, flat and rigid π-system skeleton. The addition of two types of sterically bulky protecting substituents, Tip (2,4,6-triisopropylphenyl) and *tert*-butyl (*t*-Bu) groups, were investigated. The deuterium atoms for COPV2-d_2 aimed to examine the efficacy of kinetic isotope effect for stabilization for the present purpose.

2. Experimental

Materials. Commercial reagents were purchased from Sigma-Aldrich, TCI, or Wako Pure Chemical Industries, Ltd. and used as received. COPVs were prepared according to previously reported procedures.[16]

Synthesis. All reactions were carried out under an atmosphere of nitrogen unless otherwise noted. Analytical thin-layer chromatography (TLC) was performed using glass plates precoated with 0.25 mm silica gel impregnated with a fluorescent indicator (254 nm). (Merck Millipore 105715). TLC plates were visualized by exposure to ultraviolet light (UV). Flash column chromatography was performed employing Kanto Silica gel 60 (spherical, neutral, 63–210 mesh). Preparative gel permeation column chromatography (GPC) was performed on a Japan Analytical Industry LaboACE LC-5060 (eluent: chloroform) with JAIGEL 2HR and 2.5HR. ^{1}H and ^{13}C NMR spectra were recorded on a JEOL ECA-500 or ECZ-400 spec-

trometer using tetramethylsilane as an internal standard.

Representative Procedure for COPV1-Tip. A mixture of COPV1-Br_2 (100 mg, 0.0897 mmol), $Pd_2(dba)_3$ (5 mol%), SPhos (10 mol%), K_3PO_4 (70 mol%), and $TipB(OH)_2$ (3.0 eq) in toluene (1 mL) was stirred at 100 °C for 48 h. After cooling to ambient temperature, the reaction mixture was diluted with chloroform and passed through a short plug of silica gel. The thus obtained crude mixture was subjected to preparative GPC (eluent: chloroform) to furnish **COPV1-Tip** (55 mg, 45% yield). ^{1}H NMR (500 MHz, $CDCl_3$): δ 0.85–0.90 (m, 24H), 1.06 (d, $^3J = 6.8$ Hz, 12H), 1.25–1.28 (m, 52H), 1.54–1.55 (m, 8H), 2.54 (t, $^3J = 7.4$ Hz, 8H), 2.60 (sep, $^3J = 6.9$ Hz, 4H), 2.90 (sep, $^3J = 6.8$ Hz, 2H), 6.93 (dd, $^3J = 7.4$ and $^4J = 1.1$ Hz, 2H), 7.00 (s, 4H), 7.03 (d, $^3J = 8.0$ Hz, 8H), 7.19 (d, $^4J = 1.1$ Hz, 2H), 7.22–7.24 (m, 10H), ^{13}C NMR (125 MHz, $CDCl_3$): δ 14.1, 22.7, 22.7, 23.9, 24.1, 24.4, 29.2, 29.3, 29.5, 30.1, 31.4, 31.9, 34.3, 35.5, 62.4, 120.1, 120.5, 127.3, 127.9, 128.2, 128.5, 136.9, 137.5, 137.7, 140.7,141.1, 146.8, 147.6, 155.3, 157.4.

COPV1-*t*-Bu. ^{1}H NMR (400 MHz, $CDCl_3$): δ 0.86 (t, $^3J = 6.8$ Hz, 12H), 1.22–1.29 (m, 58H), 1.51–1.58 (m, 8H), 2.53 (t, $^3J = 7.8$ Hz, 8H), 7.01 (d, $^3J = 8.2$ Hz, 8H), 7.08–7.14 (m, 4H), 7.19 (d, $^3J = 8.2$ Hz, 8H), 7.45 (d, $^4J = 1.4$ Hz, 2H), ^{13}C NMR (100 MHz, $CDCl_3$): δ 14.1, 22.7, 29.3, 29.5, 29.5, 31.3, 31.9, 34.8, 35.6, 62.5, 119.9, 122.4, 123.5, 128.1, 128.4, 136.2, 140.8, 141.1, 148.3, 154.7, 157.2.

COPV2-Tip. ^{1}H NMR (500 MHz, $CDCl_3$): δ 0.85–0.89 (m, 24H), 1.04 (d, $^3J = 6.8$ Hz, 12H), 1.26–1.28 (m, 52H), 1.49–1.54 (m, 8H), 2.47 (t, $^3J = 7.4$ Hz, 8H), 2.58 (sep, $^3J = 6.9$ Hz, 4H), 2.89 (sep, $^3J = 6.9$ Hz, 2H), 6.88–6.92 (m, 10H), 6.98 (s, 4H), 7.08 (d, $^3J = 8.6$ Hz, 8H), 7.17–7.26 (m, 16H), 7.28–7.30 (m, 8H), 7.35 (s, 2H), ^{13}C NMR (125 MHz, $CDCl_3$): δ 14.1, 22.7, 23.9, 24.1, 24.4, 29.2, 29.4, 29.5, 30.0, 31.3, 31.9, 34.2, 35.5, 62.2, 63.0, 118.1, 119.7, 120.4, 126.5, 127.2, 128.0, 128.0, 128.2, 128.8, 136.4, 137.0, 137.4, 137.6, 140.4, 141.1, 143.9, 146.8, 147.6, 154.1, 155.9, 155.9, 156.9.

COPV2-*t*-Bu. ^{1}H NMR (400 MHz, $CDCl_3$): δ 0.87 (t, $^3J = 6.8$ Hz, 12H), 1.24–1.28 (m, 94H), 1.49–1.55 (m, 8H), 2.46 (t, $^3J = 7.8$ Hz, 8H), 6.93 (d, $^3J = 8.3$ Hz, 8H), 7.13–7.19 (m, 28H), 7.28 (s, 2H), 7.51 (s, 2H), ^{13}C NMR (100 MHz, $CDCl_3$): δ 14.1, 22.7, 29.3, 29.4, 29.7, 31.3, 31.4, 31.5, 31.9, 34.3, 34.8, 35.6, 62.0, 62.4, 118.2, 120.0, 122.4, 123.6, 124.9, 128.0, 128.2, 128.4, 136.0, 136.8, 140.7, 140.9, 141.0, 148.1, 148.8, 153.9, 155.5, 156.0, 156.6.

COPV2-d_2. *n*-BuLi (3.5 eq, 1.6 M in *n*-hexane) was added dropwise at 0 °C to a solution of **COPV2-Br_2** (297 mg, 0.192 mmol) in diethyl ether (15 mL). After the reaction mixture was stirred at 0 °C for 2 h, D_2O (0.1 mL) was added and then stirred at room temperature for 1 h. The reaction was quenched with MeOH, filtered and washed with water and MeOH successively to furnish **COPV2-d_2** (222 mg, 83% yield) as yellow solid. ^{1}H NMR (600 MHz, $CDCl_3$): δ 0.88 (t, $^3J = 7.2$ Hz, 12H), 1.28–1.31 (m, 40H), 1.50–1.55 (m, 8H), 2.49 (t, $^3J = 8.1$ Hz, 8H), 6.93 (d, $^3J = 8.4$ Hz, 8H), 7.09–7.10 (m, 10H), 7.15–7.23 (m, 22H), 7.29 (s, 2H), 7.41 (s, 2H), ^{13}C NMR (150 MHz, $CDCl_3$): δ 14.1, 22.7, 29.2, 29.5, 29.6, 31.3, 31.9, 35.6, 62.3, 62.8, 118.0, 120.5, 124.9, 126.6, 126.8, 128.1, 128.2, 128.7, 136.4, 138.9, 140.1, 141.3, 143.4, 154.1, 156.0, 156.1, 157.2.

Quantum Chemical Calculations. Geometry optimization was performed on the model compounds without octyl groups to reduce the calculation cost, using density functional theory with B3LYP using 6-31G* basis on Gaussian 09.[27]

Thin Film Preparation. Thin films containing a small percentage of the COPV1 or COPV2 derivatives dispersed in PS, used as a passive matrix, were spin-coated over 2.5 × 2.5 cm^2 commercial transparent quartz plates. For a proper comparison, films with the same molar concentration were used. Dye content in the films was 3 wt% for the COPV1 and COPV2 derivatives, while for the rest of compounds the percentage was adjusted to have the same number of COPV1 or COPV2 molecules per gram of PS (that is, 323×10^{-7} and 223×10^{-7} moles of dye/gram of PS, respectively). For the COPV1 derivatives, films with 5 wt% were also prepared (and equivalent concentrations in molecules per gram of PS for the other COPV1 derivatives). The percentage of PS in the solvent (toluene) was adjusted to ensure that the films constituted waveguides supporting only fundamental transversal modes (electric and magnetic, TE_0 and TM_0, respectively), propagating with a high confinement factor ($\Gamma \approx 90\%$). This means choosing film thickness (h) values (determined from the interference pattern observed in the transparent region of the spectrum)[28] just below the cutoff thickness for the propagation of the first-order mode TE_1. Such election is convenient to minimize losses, and thus to optimize the ASE performance.[29,30]

Optical Experiments. Absorption measurements were carried out with a Jasco V-650 spectrophotometer. The absorption coefficient at a given wavelength (α_λ) was calculated according to $\alpha_\lambda = 2.3\ A_\lambda/h$, where A_λ is the absorbance at that wavelength. Room temperature photoluminescence (PL) spectra were obtained with a Jasco FP-6500 fluorimeter by exciting at a 60° angle with respect to the normal to the film. The PL emission was collected in reflection at a 30° angle to avoid the pump beam. The excitation wavelengths used in the PL measurements were 320 and 395 nm for the COPV1 and COPV2 derivatives, respectively. The PLQY was measured using an integrating sphere attached to the fluorimeter.

ASE characterization was performed under optical excitation with a light stripe (3.5 × 0.5 mm^2) incident over the sample in a perpendicular direction with respect to the film. Light emitted by the film was collected from the edge of the film with an Ocean Optics USB2000-UV-VIS fiber spectrometer (resolution 1.3 nm). The excitation source was a pulsed Nd:YAG laser (10 ns, 10 Hz) emitting at 355 nm, for the COPV1 derivatives. Such laser was used to pump an optical parametric oscillator (OPO), which was the source to excite the COPV2 derivatives. The pump wavelength (λ_{pump}) for each compound was selected in order to match a peak of maximum film absorption (λ_{pump} values and their corresponding temporal pulse widths t_p, are listed in Table S1).

3. Results and Discussion

Synthesis and Quantum Chemical Calculations. The synthesis of **COPV*n*-Tip** and **COPV*n*-*t*-Bu** was carried out by means of Pd- or Ni-catalyzed cross-coupling reaction. **COPV2-d_2** was obtained by quenching dilithiated COPV2 with D_2O. Details are shown in the Experimental section.

The calculated optimized geometries and orbital energies for the various compounds are shown in the supporting information section (Figure S1). The COPV plane and the phenyl

planes of the Tip groups are almost perpendicular with the dihedral angles of 90°, suggesting that there is no extension of the π-conjugation between those groups. The slight red-shift in the absorption spectra can be understood in terms of electronic perturbation caused by the inductive effect of the Tip group, homoconjugation and/or dipole-dipole interaction between the COPV core[31,32] and Tip groups. Installation of *t*-Bu did not significantly change the geometry of the COPV skeleton. In these compounds, the effects of the substituents on the frontier orbital energies are also very small, and the HOMO-LUMO energy differences (ΔE) are larger by 0.1 and 0.2 eV for the Tip and *t*-Bu derivatives than those of their parent compounds (Supporting Information).

Absorption, Photoluminescence and ASE Film Properties. The absorption and PL spectra for films of all the COPV derivatives used in the present study are shown in Figure 2 and all relevant parameters are listed in Table 1 (see also Table S2). For the COPV1 derivatives, which absorb in the UV region (320–370 nm), the absorption spectral shapes are similar to that of COPV1 with small redshift (9 and 5 nm for **COPV1-Tip** and **-*t*-Bu**, respectively), which are consistent with the calculated ΔE. The COPV2 derivatives, absorbing in the region of 350–420 nm, show the similar tendency. The spectrum for **COPV2-d_2** is practically the same, given that its only difference with respect to **COPV2** is the replacement of the H atoms of the terminal positions with deuterium. With regards to the PL spectra, the shapes for the various COPV1 and 2 derivatives are similar to those of **COPV1** and **COPV2**, respectively, and are shifted with respect to them, following the same trend observed in the absorption spectra. PLQY values above 90% are obtained for all the films using PS as the matrix (see Table 1). Quantitatively, it is seen that film absorption coefficients for the compounds with Tip and *t*-Bu substituents are larger than those of the parent **COPV1** or **COPV2**. To ascertain whether these are due to differences between the molecules or to different intermolecular interactions, we measured absorption (ε) in diluted liquid solutions on dichloromethane (see Figure S2, supporting information). Results indicate that the larger absorption observed in films containing **COPV1-Tip** and **COPV2-Tip** relative to that of films doped with **COPV1** and **COPV2**, respectively is because the molecule extinction coefficient ε is larger.

The potential of a given material to be used as the active medium for a waveguide-based laser device, consists in studying its ASE properties when deposited as a thin waveguide film. The presence of ASE reflects in a narrowing of the PL spectrum at a given pump intensity, accompanied by a sudden increase of the emission intensity.[3–5,33] The observation of ASE is a signature of the existence of gain due to the dominant contribution of stimulated emission over the spontaneous. The ASE spectra of the PS films containing either of the COPV1 or COPV2 derivative are shown in Figures 2a and 2b, respectively. All the compounds display a net narrowing of the PL emission with ASE peaks (λ_{ASE}) at different wavelengths. The linewidth of the ASE emission is defined as the full width at half maximum (FWHM) and is typically of several nm (see exact values in Table 1). The first interesting result is the possibility to tune λ_{ASE} over a relatively wide range by choosing a proper COPV-based dye (385–413 nm and 462–474 nm, for

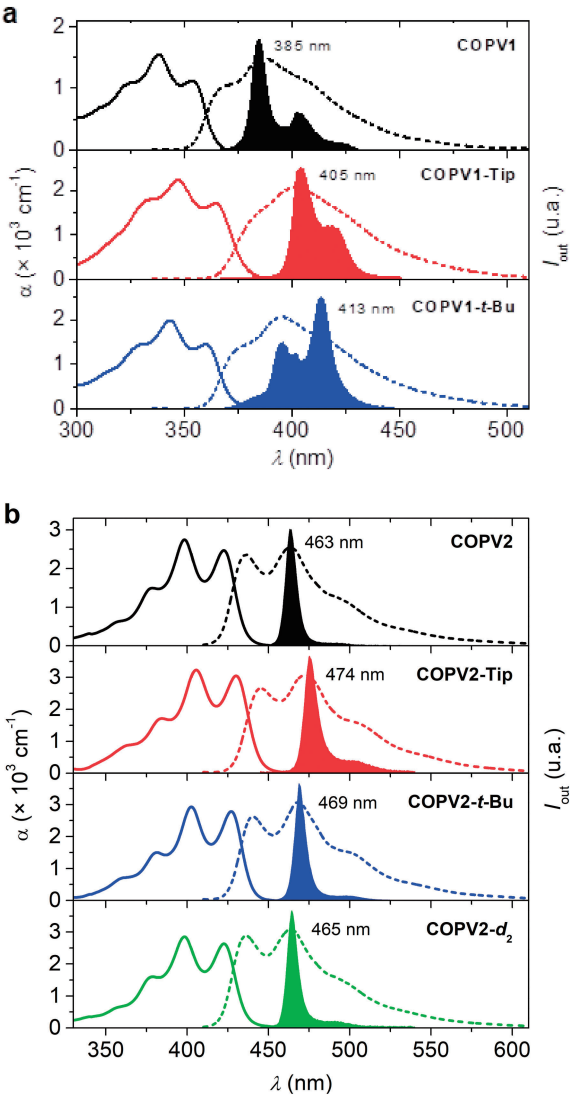

Figure 2. Optical properties at room temperature of PS films doped with (a) COPV1 derivatives and (b) COPV2 derivatives. Dye contents are 323×10^{-7} mol/gPS and 223×10^{-7} mol/gPS, for COPV1 and COPV2 derivatives, respectively. Absorption coefficient, α (solid line, left axis), photoluminescence intensity (dashed line, right axis), and amplified spontaneous emission, ASE, intensity (filled area, right axis), versus wavelength, λ.

COPV1 and COPV2 derivatives, respectively) by changing the type of peripheral substituent in the COPV. The shifts in the λ_{ASE} values are a consequence of the shifts in the ABS and PL spectra as discussed above. While the main motivation to add groups to the terminal positions is to improve the stability, these results opened a way to tune the emission wavelength of the lasers. In this regard, it should be noted, that the particular wavelength at which a given laser (based on a film with a fixed thickness and dye content) emits, is determined by the geometrical parameters of the laser resonator (mainly the grating period). But the minimum laser threshold occurs when the laser wavelength matches that at which ASE is observed because it corresponds to the wavelength at which gain is maximum.[34,35] Thus, changes in the ASE wavelength (in this case provided

Table 1. Optical and ASE parameters of PS films doped with COPV1 and COPV2 derivatives.

COPV	COPV (wt.%) in PS[a]	PLQY[b] %	$\lambda_{ABS\text{-}max}$[c] (nm)	$\lambda_{PL\text{-}max}$[d] (nm)	$\alpha[\lambda_p]$[e] ($\times 10^3$ cm^{-1})	λ_{ASE}[f] (nm)	FWHM[g] (nm)	$E_{th\text{-}ASE}$[h] (μJ/cm^2)	$I_{th\text{-}ASE}$[h] (kW/cm^2)	$\tau_{1/2}^{ASE}$ [I_{pump}][i] (pump pulses) [kW/cm^2]
1	3.0	100 ± 10	324, 338, 354	368, 385, 403	1.1	384.5	7	2500	250	1.2×10^2 [1070]
	5.0	100 ± 7			1.9	385.2	6	900	90	1.8×10^2 [200]
1-Tip	4.2	100 ± 6	334, 347, 364	383, 401, 422	1.7	404.0	12	1500	150	1.2×10^3 [200]
	6.9	96 ± 5			3.0	404.7	9	700	70	6.0×10^2 [200]
1-*t*-Bu	3.3	100 ± 8	329, 343, 360	377, 396, 415	1.4	—	—	$>1.4 \times 10^5$	$>1.4 \times 10^4$	—
	5.6	100 ± 7			2.4	413.3	11	6200	620	1.5×10^2 [1400]
2	3.0	85 ± 7	379, 398, 423	436, 461, 490	2.5	462.7	7	55	15	1.5×10^4 [40.8]
2-Tip	3.8	90 ± 7	385, 406, 430	445, 471, 503	3.1	473.8	8	40	11	1.1×10^5 [23.0] 5.5×10^4 [40.3]
2-*t*-Bu	3.7	82 ± 7	382, 403, 427	440, 466, 498	2.8	469.0	7	55	15	1.8×10^4 [27.1] 8.5×10^3 [39.7]
2-d_2	3.0	86 ± 7	379, 398, 423	436, 464, 490	2.6	465.2	7	65	17	1.9×10^4 [39.2]

[a]Error ~0.1%; [b]PLQY, photoluminescence quantum yield; [c]Peak absorption wavelengths (maximum absorption peak is underlined); [d]Peak photoluminescence wavelengths (maximum photoluminescence peak is underlined); [e]Absorption coefficient at the pump wavelength, λ_p (error ~2%); [f]ASE wavelength (error is ±0.5 nm); [g]ASE linewidth (error is ±1 nm), defined as the full width at half maximum (FWHM) above the threshold; [h]ASE threshold (error ~20%); [i]ASE operational lifetime, characterized by the photostability half-life $\tau_{1/2}^{ASE}$ (determined from Figure 4) measured at 10 Hz (error ~10%). The pump intensities are indicated in square brackets.

by the use of different derivatives) provides a way to obtain optimized lasers (i.e. with lowest possible threshold) emitting at different wavelengths.

For all the compounds, except for **COPV1-*t*-Bu**, ASE occurs very close to the first vibrational component of the PL spectrum (the 0–1), which for the COPV1 and COPV2 derivatives is the most intense one. On the other hand, for **COPV1-*t*-Bu**, ASE appears at around 413 nm, which corresponds to the 0–2 vibrational component, clearly red-shifted with respect to its maximum PL peak (observed at 396 nm). The correlation between the peaks observed in the PL spectra and the molecular vibrations was analysed in detail through Raman experiments for **COPV1** and **COPV2**.[16] In many materials investigated in the literature, ASE appears at the most intense vibronic transition. Very often this is the 0–1 transition, given that the intensity of the 0–0 component is reduced by self- or re-absorption due to the proximity between absorption and PL.[3,4] That is the case for highly planar and stable derivatives with small Stokes shift, such as perylenediimides[21,22] or COPV*n* (with $n = 1$ to 6).[7] In the meanwhile, the observation of ASE at wavelengths associated to the 0–2 PL transition has been reported in other materials.[36] Different types of mechanisms might be responsible for such behavior, such as the existence of triplet-triplet absorption or excited state absorption in the region at which the 0–1 PL transition appears.[36–41] Further photophysical studies and theoretical calculations are required to clarify this phenomenon in **COPV1-*t*-Bu**, and might be the subject of future investigations.

The ASE thresholds ($E_{th\text{-}ASE}$ and $I_{th\text{-}ASE}$, expressed in energy density and power density units, respectively) for all the films are discussed based on the results shown in Figure 3a. They were determined from plots of the emission linewidth (red curves, right axis) and those of the output intensity (blue curves, left axis) as a function of the pump intensity. Numerical $E_{th\text{-}ASE}$ (and $I_{th\text{-}ASE}$) values shown in Table 1 are obtained from the red emission linewidth curves and correspond to the pump energy (power) density at which the output intensity decays to half of its initial value. To ensure proper comparisons among different compounds, the $I_{th\text{-}ASE}$ value for each film has been represented as a function of its absorption coefficient at λ_{pump} (Figure 3b). It should be noted that the figure includes not only the data shown in Table 1 but also those obtained using the same films with a different λ_{pump}, or of other films with different dye loading amounts. It is seen that for a given compound, these parameters are inversely correlated (shown in blue line in Figure 3b), as expected whenever PL quenching due to molecular aggregation and/or interaction is negligible. Actually, such a correlation was already found independently for parent COPV1 and COPV2.[7] Interestingly, the data obtained from other COPV2 derivatives used in the present study were found to be on the same line as the parent COPV2. This sounds reasonable, taking into account that the PLQY values of the series of these COPV2 derivatives are similar. With regards to the COPV1 derivatives, **COPV1** and **COPV1-Tip** behave similarly. In sharp contrast, **COPV1-*t*-Bu** has a larger threshold with large deviation from the green line in Figure 3b, attributed to the fact that ASE appears at the second vibrational peak (instead of at the first) as discussed above.

The most relevant feature found through this study is the improved ASE photostability of some of the COPV derivatives, attributed to the protection of their terminal sites by proper substituents. This property is studied by recording the ASE intensity as a function of time (or the number of pump pulses) at a fixed pump intensity incident on the same spot of the sample. Examples of such plots are shown in Figures 4a and 4b, for various COPV1 and COPV2 compounds, respectively. Here, the parameter used to quantify this property is called ASE photostability half-life ($\tau_{1/2}^{ASE}$), defined as the time or number of pump pulses at which the ASE intensity decays to half of its initial value. Results for all the films are included in Table 1. Note that for proper comparisons of different films, the $\tau_{1/2}^{ASE}$ were obtained under the same pump intensity for each series

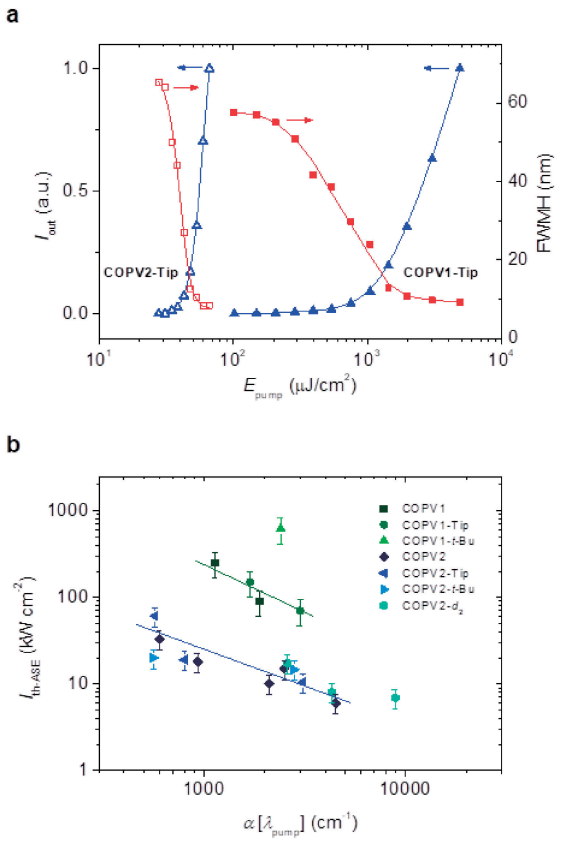

Figure 3. Amplified spontaneous emission thresholds. a) Output intensity, I_{out}, (blue triangles, left axis) and emission linewidth, FWHM, (red squares, right axis) as a function of the pump energy density, E_{pump}, for PS films doped with **COPV1-Tip** (full symbols) and **COPV2-Tip** (empty symbols) at 550×10^{-7} mol/gPS and 223×10^{-7} mol/gPS, respectively; b) ASE thresholds, $I_{th\text{-}ASE}$, versus the absorption coefficient at the pump wavelength, $\alpha[\lambda_{pump}]$, for films containing every COPV derivative (see legend). The full line is a guide to the eye to show the behavior trend for **COPV1** and **COPV1-Tip** (green line) and all COPV2 compounds (blue line).

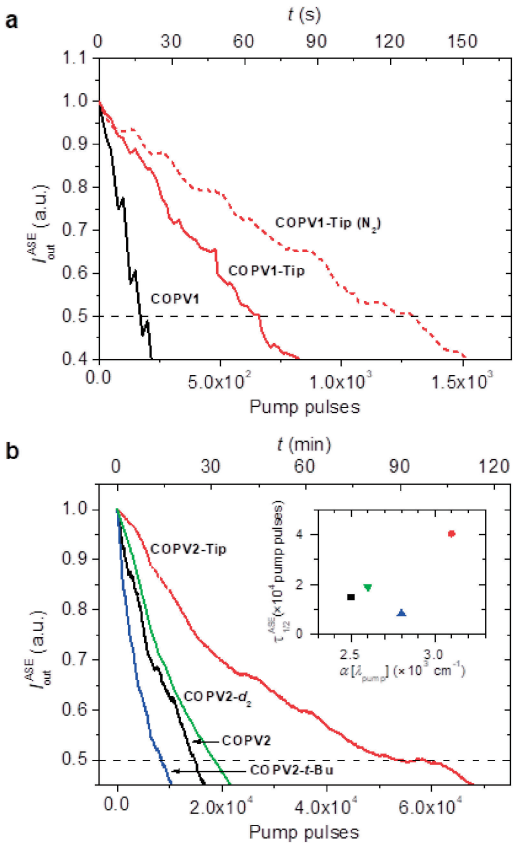

Figure 4. Amplified spontaneous emission photostability. ASE intensity, I_{out}, versus the number of pump pulses and time (bottom and top axes, respectively) for various COPV1 and COPV2 derivatives (a and b, respectively). The particular compound for each case is indicated with a label next to each curve. All measurements were carried out in air. For **COPV1-Tip**, a measurement in a N_2 atmosphere was also done. Samples were excited at 200 kW/cm^2 and 40 kW/cm^2, for COPV1 and COPV2 derivatives, respectively. The operational ASE lifetime ($\tau^{ASE}{}_{1/2}$) values indicated in Table 1 are obtained from these curves as the time (or number of pump pulses), at which I_{out} decays to half of its initial value; $\tau^{ASE}{}_{1/2}$ values for the COPV2 compounds versus the absorption coefficient at the pump wavelength, $\tau[\lambda_{pump}]$, are shown as an inset in Figure 4b.

of compounds (around 200 and 40 kW/cm^2, for the COPV1 and COPV2 derivatives respectively). Also, in order to ensure that differences are not a consequence of differences in absorption, the $\tau_{1/2}{}^{ASE}$ values are plotted as a function of the absorption coefficient in the inset of Figure 4b. In such a representation, the $\tau_{1/2}{}^{ASE}$ value of a given compound, or of compounds behaving similarly, would decrease with increasing absorbance.

From Figure 4, it is seen that films containing compounds with Tip substituents show three times larger $\tau_{1/2}{}^{ASE}$ values (recorded under ambient conditions) than those of the corresponding parent COPV1 and COPV2. Moreover, the Tip-substituted derivatives showed significantly improved stability among those used in the present study (see Figure 4 and Table 1). This is a consequence of the proper kinetic protection with the substituents added to the terminal positions, which protect the molecule from photoreaction. It should be also noted that the $\tau_{1/2}{}^{ASE}$ values of the compounds with Tip substituents doubled under a nitrogen atmosphere (see Figure 4a). This is in accordance with the previous results obtained with COPV1 and COPV6, and indicates that the photodegradation is mainly related to the presence of oxygen.[7] Remarkably, the higher photostability of the Tip-substituted compounds appears to be even better when the absorbance of the films is considered in the discussion (Figure 4b inset). It is seen that despite the larger absorbance of the film with **COPV2-Tip**, its stability is various times larger than that of **COPV2**. On the other hand, the use of *t*-Bu groups instead of Tip at the terminal positions does not seem to improve the photostability. According to the curves shown in Figure 4, it appears to be lower than that of **COPV2**, but in fact this can be attributed to the larger absorbance of the film (see Figure 4b, inset). Therefore, according to these data, their performance appears to be similar. Interestingly, data for **COPV2-*d*$_2$** indicates that the use of deuterium at the terminal positions leads also to an improved stability.

Again, looking at the inset of Figure 4b, it is seen that the apparently small improvement in **COPV2-d_2**, with respect to **COPV2** is in fact larger when absorbance is taken into account (Figure 4b, inset). Nevertheless, the stability improvement achieved with deuterium is smaller than that obtained with the TIP substituents. This suggests that the abstraction of the terminal H(D) atom is not the rate-determining step of the degradation process, because, based on the primary kinetic isotope effect, the C-D cleavage should be slowed down by a factor of ca. 6.5-times than that of C-H at ambient temperature if this step determines the rate of the whole reaction process.[42]

4. Conclusion

The synthesis of various COPV1 and COPV2 derivatives, designed to have improved stabilities with respect to previously reported COPV1 and COPV2, and the study of their optical and ASE properties, diluted in polystyrene films, have been presented here. The efficacy to prevent photodegradation by functionalizing at the terminal COPV positions with two types of sterically bulky protecting substituents, Tip (2,4,6-triisopropylphenyl) and *tert*-butyl (*t*-Bu) groups has been investigated in the compounds **COPV1-Tip** and **COPV2-Tip**; and **COPV1-*t*-Bu** and **COPV2-*t*-Bu**, respectively. Three times longer operational ASE lifetimes (recorded under ambient conditions), relative to the values of COPV1 and COPV2, have been measured for the compounds with Tip groups. On the other hand, lower ASE lifetimes have been obtained with the derivatives with *t*-Bu groups. The efficacy of kinetic isotope effect for stabilization by the addition at terminal positions of deuterium atoms has also been studied (derivative **COPV2-d_2**). The ASE lifetime for this compound is only slightly better than that of COPV2, less than expected according to the primary kinetic isotope effect, thus suggesting that the abstraction of the terminal H(D) atom is not the rate-determining step of the degradation process. Finally, it should also be remarked that the installation of substituents affects the ASE wavelength, which varies in the ranges 385–413 nm and 462–474 nm, for the investigated COPV1 and COPV2 derivatives, respectively. Thus, while the main motivation to add groups to the terminal positions was to improve the stability, these results indicate that this strategy also serves to tune the ASE wavelength.

Financial support from Spanish Ministerio de Economía y Competitividad (MINECO) and the European FEDER funds through Grant MAT2015-66586-R is gratefully acknowledged. We also thank V. Esteve for technical assistance. This work was partially supported by MEXT and JSPS KAKENHI Grant Numbers JP16H04106 and JP19H05716 to HT and JP19H0549 to EN.

Supporting Information

Details of photophysical property measurements and calculations. This material is available on https://doi.org/10.1246/bcsj.20200042.

References

1 Y. Shirota, H. Kageyama, *Chem. Rev.* **2007**, *107*, 953.
2 Y. Geerts, K. Müllen, Advanced Light Emitting Dyes: Monomers, Oligomers, and Polymers. In *Applied Fluorescence in Chemistry, Biology and Medicine*; Springer-Verlag Berlin Heidelberg, 1999; pp. 299–324.
3 S. Chénais, S. Forget, *Polym. Int.* **2012**, *61*, 390.
4 A. J. C. Kuehne, M. C. Gather, *Chem. Rev.* **2016**, *116*, 12823.
5 M. Anni, S. Lattante, *Organic Lasers: Fundamentals, Developments, and Applications*; Pan Stanford Publishing: Singapore, 2018.
6 A. S. D. Sandanayaka, T. Matsushima, F. Bencheikh, S. Terakawa, W. J. Potscavage, Jr., C. Qin, T. Fujihara, K. Goushi, J.-C. Ribierre, C. Adachi, *Appl. Phys. Express* **2019**, *12*, 061010.
7 M. Morales-Vidal, P. G. Boj, J. M. Villalvilla, J. A. Quintana, Q. Yan, N. T. Lin, X. Zhu, N. Ruangsupapichat, J. Casado, H. Tsuji, E. Nakamura, M. A. Díaz-García, *Nat. Commun.* **2015**, *6*, 8458.
8 V. Bonal, R. Muñoz-Mármol, F. Gordillo Gámez, M. Morales-Vidal, J. M. Villalvilla, P. G. Boj, J. A. Quintana, Y. Gu, J. Wu, J. Casado, M. A. Díaz-García, *Nat. Commun.* **2019**, *10*, 3327.
9 F. Hide, M. A. Díaz-García, B. J. Schwartz, M. R. Andersson, Q. Pei, A. J. Heeger, *Science* **1996**, *273*, 1833.
10 N. Tessler, G. J. Denton, R. H. Friend, *Nature* **1996**, *382*, 695.
11 K. P. Kretsch, C. Belton, S. Lipson, W. J. Blau, F. Z. Henari, H. Rost, S. Pfeiffer, A. Teuschel, H. Tillmann, H. H. Hörhold, *J. Appl. Phys.* **1999**, *86*, 6155.
12 R. E. Martin, F. Diederich, *Angew. Chem., Int. Ed.* **1999**, *38*, 1350.
13 S. Kubatkin, A. Danilov, M. Hjort, J. Cornil, J. L. Brédas, N. Stuhr-Hansen, P. Hedegård, T. Bjørnholm, *Nature* **2003**, *425*, 698.
14 M. A. Díaz-García, E. M. Calzado, J. M. Villalvilla, P. G. Boj, J. A. Quintana, F. Giacalone, J. L. Segura, N. Martín, *J. Appl. Phys.* **2005**, *97*, 063522.
15 V. K. Praveen, C. Ranjith, E. Bandini, A. Ajayaghosh, N. Armaroli, *Chem. Soc. Rev.* **2014**, *43*, 4222.
16 X. Zhu, H. Tsuji, J. T. López Navarrete, J. Casado, E. Nakamura, *J. Am. Chem. Soc.* **2012**, *134*, 19254.
17 P. M. Burrezo, N.-T. Lin, K. Nakabayashi, S. Ohkoshi, E. M. Calzado, P. G. Boj, M. A. Díaz-García, C. Franco, C. Rovira, J. Veciana, M. Moos, C. Lambert, J. T. López-Navarrete, H. Tsuji, E. Nakamura, J. Casado, *Angew. Chem., Int. Ed.* **2017**, *56*, 2898.
18 H. Tsuji, E. Nakamura, *Acc. Chem. Res.* **2019**, *52*, 2939.
19 E. Y. Choi, L. Mazur, L. Mager, M. Gwon, D. Pitrat, J. C. Mulatier, C. Monnereau, A. Fort, A. J. Attias, K. Dorkenoo, J. E. Kwon, Y. Xiao, K. Matczyszyn, M. Samoc, D.-W. Kim, A. Nakao, B. Heinrich, D. Hashizume, M. Uchiyama, S. Y. Park, F. Mathevet, T. Aoyama, C. Andraud, J. W. Wu, A. Barsella, J. C. Ribierre, *Phys. Chem. Chem. Phys.* **2014**, *16*, 16941.
20 F. Laquai, A. K. Mishra, M. R. Ribas, A. Petrozza, J. Jacob, L. Akcelrud, K. Müllen, R. H. Friend, G. Wegner, *Adv. Funct. Mater.* **2007**, *17*, 3231.
21 M. G. Ramírez, M. Morales-Vidal, V. Navarro-Fuster, P. G. Boj, J. A. Quintana, J. M. Villalvilla, A. Retolaza, S. Merino, M. A. Díaz-García, *J. Mater. Chem. C* **2013**, *1*, 1182.
22 M. G. Ramírez, S. Pla, P. G. Boj, J. M. Villalvilla, J. A. Quintana, M. A. Díaz-García, F. Fernández-Lázaro, Á. Sastre-Santos, *Adv. Opt. Mater.* **2013**, *1*, 933.
23 P. M. Burrezo, X. Zhu, S.-F. Zhu, Q. Yan, J. T. López Navarrete, H. Tsuji, E. Nakamura, J. Casado, *J. Am. Chem. Soc.* **2015**, *137*, 3834.
24 M. Morales-Vidal, J. A. Quintana, J. M. Villalvilla, P. G.

Boj, H. Nishioka, H. Tsuji, E. Nakamura, G. L. Whitworth, G. A. Turnbull, I. D. W. Samuel, M. A. Díaz-García, *Adv. Opt. Mater.* **2018**, *6*, 1800069.
25 H. Nishioka, H. Tsuji, E. Nakamura, *Macromolecules* **2018**, *51*, 2961.
26 S. Watanabe, K. Yamanishi, H. Tsuji, *ChemPhotoChem* **2019**, *3*, 605.
27 Gaussian 09, Revision E.01, M. J. Frisch et al., Gaussian, Inc., Wallingford CT, 2013.
28 V. Bonal, J. A. Quintana, R. Muñoz-Mármol, J. M. Villalvilla, P. G. Boj, M. A. Díaz-García, *Thin Solid Films* **2019**, *692*, 137580.
29 E. M. Calzado, M. G. Ramírez, P. G. Boj, M. A. Díaz-García, *Appl. Opt.* **2012**, *51*, 3287.
30 M. Anni, A. Perulli, G. Monti, *J. Appl. Phys.* **2012**, *111*, 093109.
31 J. Sukegawa, H. Tsuji, E. Nakamura, *Chem. Lett.* **2014**, *43*, 699.
32 Q. Yan, Y. Guo, A. Ichimura, H. Tsuji, E. Nakamura, *J. Am. Chem. Soc.* **2016**, *138*, 10897.
33 I. D. W. Samuel, E. B. Namdas, G. A. Turnbull, *Nat. Photonics* **2009**, *3*, 546.
34 M. G. Ramirez, P. G. Boj, V. Navarro-Fuster, I. Vragovic, J. M. Villalvilla, I. Alonso, V. Trabadelo, S. Merino, M. A. Díaz-García, *Opt. Express* **2011**, *19*, 22443.
35 V. Navarro-Fuster, I. Vragovic, E. M. Calzado, P. G. Boj, J. A. Quintana, J. M. Villalvilla, A. Retolaza, A. Juarros, D. Otaduy, S. Merino, M. A. Díaz-García, *J. Appl. Phys.* **2012**, *112*, 043104.
36 J. Casado, V. Hernández, J. T. López Navarrete, M. Algarra, D. A. da Silva Filho, S. Yamaguchi, R. Rondão, J. S. Seixas de Melo, V. Navarro-Fuster, P. G. Boj, M. A. Díaz-García, *Adv. Opt. Mater.* **2013**, *1*, 588.
37 R. Kabe, H. Nakanotani, T. Sakanoue, M. Yahiro, C. Adachi, *Adv. Mater.* **2009**, *21*, 4034.
38 M. Polo, A. Camposeo, S. Tavazzi, L. Raimondo, P. Spearman, A. Papagni, R. Cingolani, D. Pisignano, *Appl. Phys. Lett.* **2008**, *92*, 083311.
39 P. A. Losio, C. Hunziker, P. Günter, *Appl. Phys. Lett.* **2007**, *90*, 241103.
40 M. Nagawa, R. Hibino, *Appl. Phys. Lett.* **2002**, *80*, 544.
41 D. Fichou, S. Delysse, J.-M. Nunzi, *Adv. Mater.* **1997**, *9*, 1178.
42 H. Tsuji, C. Mitsui, E. Nakamura, *Chem. Commun.* **2014**, *50*, 14870.